

Comparative analysis of optimal power flow in renewable energy sources based microgrids

Raheel Muzzammel¹, Rabia Arshad¹, Sobia Bashir², Uzma Mushtaq^{3,4}, Fariha Durrani¹, Sadaf Noshin⁴

¹Department of Electrical Engineering, Faculty of Engineering and Technology, University of Lahore, Lahore, Pakistan

²School of Informatics, University of Skövde, Skövde, Sweden

³Department of Electrical and Computer Engineering, Faculty of Engineering, COMSATS Institute of Information Technology, Lahore, Pakistan

⁴Department of Technology, Faculty of Engineering and Technology, University of Lahore, Lahore, Pakistan

Article Info

Article history:

Received Jul 30, 2021

Revised Sep 29, 2022

Accepted Oct 25, 2022

Keywords:

IEEE-14 bus system

Microgrid

Newton–Raphson method

Particle swarm optimization

Renewable energy

ABSTRACT

Adaptation of renewable energy is inevitable. The idea of microgrid offers integration of renewable energy sources with conventional power generation sources. In this research, an operative approach was proposed for microgrids comprising of four different power generation sources. The microgrid is a way that mixes energy locally and empowers the end-users to add useful power to the network. IEEE-14 bus system-based microgrid was developed in MATLAB/Simulink to demonstrate the optimal power flow. Two cases of battery charging and discharging were also simulated to evaluate its realization. The solution of power flow analysis was obtained from the Newton–Raphson method and particle swarm optimization method. A comparison was drawn between these methods for the proposed model of the microgrid on the basis of transmission line losses and voltage profile. Transmission line losses are reduced to about 17% in the case of battery charging and 19 to 20% in the case of battery discharging when system was analyzed with the particle swarm optimization. Particle swarm optimization was found more promising for the deliverance of optimal power flow in the renewable energy sources-based microgrid.

This is an open access article under the [CC BY-SA](https://creativecommons.org/licenses/by-sa/4.0/) license.



Corresponding Author:

Raheel Muzzammel

Department of Electrical Engineering, Faculty of Engineering and Technology, University of Lahore

KM Off Defense Road, Lahore 54000, Pakistan

Email: raheelmuzzammel@gmail.com

1. INTRODUCTION

In the previous era when only the main grid systems were used, the end consumers often suffered because of the fault condition that occurred in the main grid. It had to be shut down and there was no backup source to provide energy. The microgrid has solved this problem because it can work in island mode. When the technology became developed and environment friendly, the distributed generation (DG) units such as wind energy, gas, and solar energy were broadly used [1]–[7]. Nowadays, the world is giving attention to the micro grid for providing energy easily and near to the load. When energy is made from natural resources like wind, bio-gas, and through sunlight (solar), there will be a very good impact on budget and also have benefit in respect of multiplicity of energy use particularly for developing countries like Pakistan [7]–[11]. While supplying energy to feeders, some feeders will have complex loads, and the provision of local energy is essential for reliability. These feeders are island from the grid using a device named static switch that can be detached in less than a cycle [12], [13]. In this condition, suitable frequency and voltages should be maintained for proper working. Whenever there will be a problem with the main grid system the static switch

will open and will start isolating the sensitive loads from the main grid system. The point where these two are attached is called the point of common coupling [14], [15]. The disturbances can also occur while switching. In this case, the distributed energy resources will restart the island mode. So, sufficient generation should be assumed to encounter the demand of loads.

Many studies have been done freshly which emphasizes the unique features of the microgrid. A group studies optimal power-sharing of disseminated generation such as wind or solar [16]–[18]. Another group researches and highlights the income of the economy. They want to reduce the overall cost of energy [19]. Another goal is to obtain extreme profit by the generation of energy. The third group of researchers determines the best communication of energy storage devices [20]–[22]. Energy can easily be stored when renewable power is present or transferring energy from one point to another point is low-priced, then the stored energy is available for the time when we cannot meet our demands or when we do not have access to renewable energy sources. The main objective is to produce low-priced energy and take advantage of renewable energy resources and the availability of energy at all times. For example, Brekken *et al.* [14] reports a wind farm rewarded by battery energy storage. Levron and Shmilovitz [23] showed storage to time-shift the production of renewables. In [24], [25], the storage devices operated in a mode of power generation. In [26], a Newton method is used to solve optimal power flow equations. The drawbacks of this method are the output results they obtained are quite near to their limits. The optimal power flow will incline variables to pass the limits and it is not reasonable to apply optimal power flow without scattered methods.

In [27], the linear programming method is proposed for optimal power flow solution [28], [29]. This method is very good in the management of inequalities and also deals very worthy with local constraints. The linear programming method is very fast and a trustworthy method for optimal power flow solutions. This method also has some demerits as it has low accuracy and the cost minimization in this method is not so good [30]. An efficient method is proposed known as the interior point method. This method took a very good benefit in the speed of convergence of 12:1 as compared to other programming methods. This method is selected for optimal power flow due to its consistency, accurateness, and quickness. There are some boundaries due to starting and ending conditions and this method does not provide a reasonable solution if the step size is chosen inappropriately. In [31], the genetic algorithm is proposed which can provide overall optimum solutions because of avoiding the setup of local minima. The main advantage of this method is to do several objectives in a solo run as it can find solutions in many areas of search space at a time. If the solution demands to work on a parallel workstation, then this method is feasible to code. The solution obtained from the genetic algorithm is not definite to be ideal and there is an excess of wastage of computational efforts in this method if power system is expanding.

All the research and studies undertake minor network topology. They should consider storage devices in a combined manner with a general proper network, but they did not. The best solution for an interconnected network with storage devices has not been shown. However, metaheuristic techniques-based implementation of microgrids is available in literature [32]–[35]. Following are the major contributions of this research.

- IEEE-14 bus system based microgrid test model is developed and is tested under different scenarios.
- The phenomena of battery charging and discharging is analyzed with this model for effective utilization of energy storage without compromise on voltage profile.
- Optimal power flow is implemented with Newton–Raphson method and particle swarm optimization (PSO) and both of these techniques are compared on the basis of voltage profile and transmission losses.
- This research serves as a study of microgrids with the integration of renewable energy and conventional energy sources.
- PSO comes up with a very good convergence speed and can control the balance between the global and local survey of search pace. This method also can deal with non-curved and non-distinguishable objective functions.

In this research, a method for making a microgrid is proposed from renewable energy resources i.e., wind and solar to supply energy in local means to end consumers [36]. If you look at the transmission lines in our country, they are too long and too old to supply energy to the end loads. Therefore, placing a microgrid near the load is a good approach. If any fault occurs at any point, then the whole area will be affected until the engineers will remove the fault. So, if we have a microgrid then we can use energy from it by dispatching it from the main grid. The power flow analysis has done by two different techniques. The first one is Newton–Raphson and the other is PSO. After comparing the results from both techniques, notice that the results from the PSO method are far better than that of Newton–Raphson.

The rest of the paper is organized as: section 2 contains the details of the formulation of the optimal power flow problem in microgrids. Section 3 explains the structure of the IEEE-14 bus system-based microgrid. Section 4 covers the discussion related to simulations. Significance of results and simulations is

mentioned in section 5. Performance of different power flow techniques is compared in section 6. Conclusions are drawn in section 7.

2. OPTIMAL POWER FLOW PROBLEM FORMULATION

Power flow is used to analyze steady-state performance. The optimization of power flow can improve performance. According to optimization, the objective function should provide the best values of power flow within the equality and inequality constraints [37]. The optimal power flow problem is (1).

$$\text{Min } F(P_G) = f(x, u) = j(x, u) \quad (1)$$

2.1. Objective function

The quadratic nature of the objective function is defined. The objective function is linked to power generation values. The objective function is given a (2),

$$J = F(P_G) \sum_{i=1}^{N_G} (P_{Gi}) = \sum_{i=1}^{N_G} (a_i + \beta_i P_{Gi} + \gamma_i P_{Gi}^2) \quad (2)$$

subjected to:

$g(x, u) = 0$ represents equality constraints.

$h(x, u) \leq$ represents inequality constraints.

$$X^T = [P_{G1}, V_{L1} \dots V_{LN_D}, Q_{G1} \dots Q_{GN_G}, S_{L1} \dots S_{LN_L}] \quad (3)$$

where X is the vector of the dependent variable which consist of slack bus power (P_G), load bus voltage (V_L), generator reactive power outputs (Q_G) and transmission line loadings (S_L); and N_L represents the number of load busses and N_G represents the number of generators.

U is the vector of independent variables which consist of voltages of the generator, transformer tap settings, and shunt compensations. Hence, u can be expressed as (4),

$$u^T = [V_{G1} \dots V_{GN_G}, P_{G2} \dots P_{GN_G}, T_1 \dots T_{NT}, Q_{C1} \dots Q_{CNC}] \quad (4)$$

where NT is the number of regulating transformers and NC is the number of shunt compensators. J is objective function to minimize and g represents here the equality constraints.

2.2. Inequality constraints responding to the limits

The generator and transformer are subjected to various types of inequality constraints. The generating voltages, active power, and reactive power are all limited. Similarly, limits are set on the transformer's control level.

– Generator:

$$V_{imin} \leq V_i \leq V_{imax}, \quad i = 1, \dots, N, \quad (5)$$

$$P_{Gimin} \leq Q_{Gi} \leq P_{Gimax}, \quad i = 1, \dots, N_G \quad (6)$$

$$Q_{gimin} \leq Q_{gi} \leq Q_{gimax}, \quad i = 1, \dots, N_g \quad (7)$$

Where V_{imin} is the minimum voltage of the generator, V_{imax} is the maximum voltage of the generator, P_{Gimin} is the minimum active power of the generator, P_{Gimax} is the maximum active power of the generator, Q_{gimin} is the minimum reactive power of the generator, and Q_{gimax} is the maximum reactive power of the generator.

– Transformer:

$$T_{kmin} \leq T_k \leq T_{kmax} \quad i = 1 \dots, N_k \quad (8)$$

where T_{kmin} is the minimum control level of the transformer and T_{kmax} is the maximum control level of the transformer.

2.3. Equations of load flow by network equality constraints

Active and reactive power are also subject to equality constraints. The equations are modelled using known parameters (voltage and angles). Normally, the difference between generation and load is expressed in the form of equality constraints. The equations are given as (9) to (10),

$$P_i(V, \delta) - P_{Gi} + P_{Di} = 0 \quad (9)$$

$$Q_i(V, \delta) - Q_{Gi} + Q_{Di} = 0 \quad (10)$$

where:

$$P_i(V, \delta) = |a| \sum_{i=1}^N |V_i| |Y_{ij}| \cos(\delta_i - \delta_j - \phi_{ij}) \quad (11)$$

$$Q_i(V, \delta) = |a| \sum_{i=1}^N |V_i| |Y_{ij}| \sin(\delta_i - \delta_j - \phi_{ij}) \quad (12)$$

$$Y_{ij} = |Y_{ij}| \phi_{ij} \quad (13)$$

The load balance equation is:

$$\sum_{i=1}^{N_G} (P_{Gi}) - \sum_{i=1}^{N_D} (P_{Di}) - P_l = 0. \quad (14)$$

2.4. Particle swarm optimization

It starts with the group of random particles and then searches for the optimal solution by updating its generations. In each or every iteration each particle is updated by two best values the first one is the position vector of the particle which had achieved so far, and it stored the value this position is called *Pbest*.

$$Pbest_i = (x_i^{best}, \dots, x_n^{best}) \quad (15)$$

Another best position is tracked by particle swarm optimizer, and it is the best solution so far by any particle in population and this position is global best which is known as *Gbest*.

$$Gbest_i = (x_i^{best}, \dots, x_n^{best}) \quad (16)$$

Velocity and position equations are given as (17) and (18).

$$v_i^k = w_i^k + c_1 r_1 (Pbest_i^k - x_i^k) + c_2 r_2 (Gbest_i^k - x_i^k) \quad (17)$$

$$x_i^{k+1} = x_i^k + v_i^{k+1} \quad (18)$$

The velocity of the i^{th} particle at the k^{th} iteration is v_i^k and x_i^k is the current position of i^{th} particle at k^{th} iteration.

- c_1 and c_2 are positive constants.
- r_1 and r_2 are two random variables with a uniform distribution between 0 and 1.
- V represents the velocity of the particle in search space.

$$V_I = (v_i, \dots, v_N)$$

- X represents the position of the particle in a search space.

$$X_I = (x_i, \dots, x_N)$$

- The upper bound is placed on the velocity in all dimensions v_{max}

$$v^{Maximum} = (X^{Maximum} - X^{Minimum})/N$$

- Here N represents the total number of intervals.

- ω is the inertia (shows the effect of previous velocity vector on the new vector).

$$\omega(K) = \omega_{maximum} - \frac{(\omega_{maximum} - \omega_{minimum}) * K}{M}$$

K represents the current number of iterations and the M represents the maximum number of iterations.

2.5. Newton–Raphson method

Newton–Raphson method is a quite efficient method for solving power flow equations [38]–[40]. This method can easily deal with large power systems because in this method the number of iterations required is independent of power system size. It is a complex system and requires more functional iterations at each step.

- Apparent power:

$$P_i - JQ_i = |V_i| < \delta_i \sum_{j=1}^n |Y_{ij}| |V_j| \angle \theta_{ij} + \delta_j \quad (19)$$

- Real part:

$$P_i = \sum_{j=1}^n |Y_{ij}| |V_j| |V_i| \cos(\theta_{ij} - \delta_i + \delta_j) \quad (20)$$

- Imaginary part:

$$Q_i = - \sum_{j=1}^n |Y_{ij}| |V_j| |V_i| \sin(\theta_{ij} - \delta_i + \delta_j) \quad (21)$$

Both (20) and (21) have algebraic equations which are nonlinear per unit values. Jacobian matrix is formulated using (22).

$$\begin{bmatrix} \Delta P \\ \Delta Q \end{bmatrix} = \begin{bmatrix} J_1 & J_2 \\ J_3 & J_4 \end{bmatrix} \begin{bmatrix} \Delta \delta \\ \Delta |V| \end{bmatrix} \quad (22)$$

Where J_1 is the order of $(n-1) \times (n-1)$, J_2 is the order of $(n-1) \times (n-1-m)$, J_3 is the order of $(n-1) \times (n-1-m)$, and J_4 is the order of $(n-1-m) \times (n-1-m)$

- The diagonal and off-diagonal elements of J_1

$$\frac{\partial P_i}{\partial \delta_i} = \sum_{j \neq i} |Y_{ij}| |V_j| |V_i| \sin(\theta_{ij} - \delta_i + \delta_j) \quad (23)$$

$$\frac{\partial P_i}{\partial \delta_j} = -|Y_{ij}| |V_j| |V_i| \cos(\theta_{ij} - \delta_i + \delta_j) \quad (24)$$

- The diagonal and off-diagonal elements of J_2

$$\frac{\partial P_i}{\partial |V_i|} = 2|Y_{ii}| |V_i| \cos \theta_{ii} + \sum_{j \neq i} |Y_{ij}| |V_j| \cos(\theta_{ij} - \delta_i + \delta_j) \quad (25)$$

$$\frac{\partial P_i}{\partial |V_j|} = |Y_{ij}| |V_j| \cos(\theta_{ij} - \delta_i + \delta_j) \quad j \neq i \quad (26)$$

- The diagonal and off-diagonal elements of J_3

$$\frac{\partial Q_i}{\partial \delta_i} = \sum_{j \neq i} |Y_{ij}| |V_j| |V_i| \cos(\theta_{ij} - \delta_i + \delta_j) \quad (27)$$

$$\frac{\partial Q_i}{\partial \delta_j} = -|V_i| |Y_{ij}| |V_j| \cos(\theta_{ij} - \delta_i + \delta_j) \quad j \neq i \quad (28)$$

- The diagonal and off-diagonal elements of J_4

$$\frac{\partial P_i}{\partial |V_i|} = -2|Y_{ii}| |V_i| \sin \theta_{ii} - \sum_{j \neq i} |Y_{ij}| |V_j| \sin(\theta_{ij} - \delta_i + \delta_j) \quad (29)$$

$$\frac{\partial P_i}{\partial |V_j|} = -|V_i||Y_{ij}|\sin(\theta_{ij} - \delta_i + \delta_j) \quad j \neq i \quad (30)$$

– Power residuals:

$$\Delta P_i^{(K)} = P_i^{sch} - P_i^{(K)} \quad (31)$$

$$\Delta Q_i^{(K)} = Q_i^{sch} - Q_i^{(K)} \quad (32)$$

In (31) and (32), these values are the differences between calculated and scheduled values. New approximations for bus voltages:

$$\delta_i^{(k+1)} = \delta_i^{(k)} + \Delta \delta_i^{(k)} \quad (33)$$

$$|V_1^{(K+1)}| = |V_1^K| + \Delta |V_1^K|. \quad (34)$$

In the case of renewable energy, power flow changes quickly. Therefore, it is advisable to find the change of power in two-time intervals instead of evaluation power mismatches at one time period. Hence, Jacobian matrix could be assumed to be constant calculated from the previous time and is given in (35).

$$\begin{bmatrix} \Delta P \\ \Delta Q \end{bmatrix} = \begin{bmatrix} J_1(t-1) & J_2(t-1) \\ J_3(t-1) & J_4(t-1) \end{bmatrix} \begin{bmatrix} \Delta \delta \\ \Delta V \end{bmatrix} \quad (35)$$

The change of power at bus k would have a direct influence on neighboring buses i.e., bus $k-1$ and bus $k+1$. Jacobian power flow equations under $N \neq k$ and $N = k$ are formulated respectively as (36) and (37).

$$\begin{aligned} \Delta P_k &= \begin{bmatrix} \frac{\partial P_k}{\partial \delta_{k-1}} & \frac{\partial P_k}{\partial \delta_k} & \frac{\partial P_k}{\partial \delta_{k+1}} \end{bmatrix} \begin{bmatrix} \Delta \delta_{k-1} \\ \Delta \delta_k \\ \Delta \delta_{k+1} \end{bmatrix} + \begin{bmatrix} \frac{\partial P_k}{\partial V_{k-1}} & \frac{\partial P_k}{\partial V_k} & \frac{\partial P_k}{\partial V_{k+1}} \end{bmatrix} \begin{bmatrix} \Delta V_{k-1} \\ \Delta V_k \\ \Delta V_{k+1} \end{bmatrix} \\ \Delta Q_k &= \begin{bmatrix} \frac{\partial Q_k}{\partial \delta_{k-1}} & \frac{\partial Q_k}{\partial \delta_k} & \frac{\partial Q_k}{\partial \delta_{k+1}} \end{bmatrix} \begin{bmatrix} \Delta \delta_{k-1} \\ \Delta \delta_k \\ \Delta \delta_{k+1} \end{bmatrix} + \begin{bmatrix} \frac{\partial Q_k}{\partial V_{k-1}} & \frac{\partial Q_k}{\partial V_k} & \frac{\partial Q_k}{\partial V_{k+1}} \end{bmatrix} \begin{bmatrix} \Delta V_{k-1} \\ \Delta V_k \\ \Delta V_{k+1} \end{bmatrix} \end{aligned} \quad (36)$$

$$\begin{aligned} \Delta P_k &= \begin{bmatrix} \frac{\partial P_k}{\partial \delta_{k-1}} & \frac{\partial P_k}{\partial \delta_k} \end{bmatrix} \begin{bmatrix} \Delta \delta_{k-1} \\ \Delta \delta_k \end{bmatrix} + \begin{bmatrix} \frac{\partial P_k}{\partial V_{k-1}} & \frac{\partial P_k}{\partial V_k} \end{bmatrix} \begin{bmatrix} \Delta V_{k-1} \\ \Delta V_k \end{bmatrix} \\ \Delta Q_k &= \begin{bmatrix} \frac{\partial Q_k}{\partial \delta_{k-1}} & \frac{\partial Q_k}{\partial \delta_k} \end{bmatrix} \begin{bmatrix} \Delta \delta_{k-1} \\ \Delta \delta_k \end{bmatrix} + \begin{bmatrix} \frac{\partial Q_k}{\partial V_{k-1}} & \frac{\partial Q_k}{\partial V_k} \end{bmatrix} \begin{bmatrix} \Delta V_{k-1} \\ \Delta V_k \end{bmatrix} \end{aligned} \quad (37)$$

The steps for Newton–Raphson are:

- a. For load buses:
 - P_i^{sch} and Q_i^{sch} are specified.
 - Voltages $|V_1^{(0)}|$ is set equal to 1.0 (slack bus value).
 - Phase angle $\delta_i^{(0)}$ is set to 0.0 (slack bus value).
 - $P_i^{(K)}$ and $Q_i^{(K)}$ are calculated from (20) and (21).
 - $\Delta P_i^{(K)}$ and $\Delta Q_i^{(K)}$ are calculated from (31) and (32).
- b. For voltage-controlled buses: $P_i^{(K)}$ and $\Delta P_i^{(K)}$ are calculated from (20) and (31).
- c. Now Jacobian matrix is obtained from (23)–(30).
- d. After obtaining the Jacobian matrix put all the values in (22) and solve this equation directly.
- e. From (33) and (34), calculate the new voltages and phase angles.
- f. The process will continue until $\Delta P_i^{(K)}$ and $\Delta Q_i^{(K)}$ are become less than the stated accuracy, i.e.

$$|\Delta Q_i^{(K)}| \leq \epsilon$$

$$|\Delta P_i^{(K)}| \leq \epsilon$$

2.6. Constraints of renewable energy sources

In this proposed work, the constraints of the renewable energy sources are met by maximum power point tracking algorithm. The power acquired from the solar photovoltaic (PV) arrays are dependent upon insolation and temperature. Nonlinear characteristics curves are obtained for voltage current relation and voltage–power relation. During the variation of insolation conditions, maximum power point should be tracked for efficient extraction of solar energy from PV arrays.

Similarly, the amount of energy that can be extracted from wind are dependent upon wind speed and tip speed ratio. As the wind speed varies, the maximum energy can be extracted by tracking the maximum power point so that the rotational speed should be varied to maintain optimal value of tip speed ratio all the time. Perturbation and observation-based method is implemented for maximizing energy from renewable energy sources [30].

2.7. Mathematical formulation of integration of renewable energy sources in the load flow

Renewable energy sources based on solar and wind are developed and implemented in this study. The beta and Weibull distribution functions are covered in the mathematical modelling of a solar PV farm and a wind farm, respectively. The variables of mathematical formulations are wind speed and solar irradiance.

2.7.1. Solar PV farm modelling

Beta distribution function is used to model probabilistic approach for solar farm [41], [42]. Therefore, solar irradiance distribution function is given (38).

$$f_b = \frac{\Gamma(\alpha+\beta)}{\Gamma(\alpha)\Gamma(\beta)} s^{(\alpha-1)}(1-s)^{(\beta-1)}; 0 \leq s \leq 1; \alpha, \beta \geq 0 \quad (38)$$

The parameters of Beta distribution are calculated as:

$$\beta = (1 - \mu) \left(\frac{\mu(1+\mu)}{\sigma^2} - 1 \right) \quad \text{and} \quad \alpha = \frac{\mu\beta}{1-\mu} \quad (39)$$

where Γ is the gamma function, s is the random variable of solar irradiance in kW/m^2 . α and β are the parameters of beta distribution function respectively, μ and σ are the mean and standard deviation of s .

2.7.2. Wind farm modelling

Weibull distribution function is used to model wind farm [41], [43]. The wind probability function is given by (40),

$$f_v(v) = \left(\frac{k}{c} \right) \cdot \left(\frac{v}{c} \right)^{(k-1)} \cdot e^{-\left(\frac{v}{c} \right)^k} \quad (40)$$

where k, c are the shape factor, scalar factor of the Weibull distribution function. The output of a wind turbine for a particular speed is given by (41),

$$P_{wr} = \begin{cases} 0 & v < v_{in} \text{ or } v > v_{out} \\ a * v^3 + b * P_r & v_{in} \leq v \leq v_r \\ P_r & v_r \leq v \leq v_{out} \end{cases} \quad (41)$$

while $a = \frac{P_r}{(v_r^3 - v_{in}^3)}$ and $b = \frac{v_{in}^3}{(v_r^3 - v_{in}^3)}$ are the constants. v_{in} , v_{out} and v_r are the cut-in, cut-out and rated speeds, respectively. The expected output power is given by (42),

$$P_{we} = P_{wr} \times f_v(v) \quad (42)$$

where P_{we} and P_{wr} are the expected output power and rated output power.

3. IEEE-14 BUS SYSTEM-BASED MICROGRID SYSTEM

In this study, a test mode for the microgrid using the IEEE 14 bus system is established. Over this test system, power flow is examined. The line data and bus data make up the test system. The line parameters of this bus system are given in Table 1.

Table 1 shows the line specifications of the 14-bus system to be designed. R and X give the resistance and inductive reactance respectively while the B/2 gives the half-line charging susceptance. Since the system is considered a microgrid, not a long transmission line, and the system is dealing with few megawatts of power, therefore the factor of capacitance is removed for better simulation results and better load flow. Figure 1 gives the MATLAB/Simulink model constructor of a microgrid.

Table 1. Line parameters

Receiving Bus	Sending bus	R (pu)	X (pu)	Half B (pu)
1	2	0.01938	0.05917	0.0264
1	5	0.05403	0.22304	0.0246
2	3	0.04699	0.19797	0.0219
2	4	0.05811	0.17632	0.017
2	5	0.05695	0.17388	0.0173
3	4	0.06701	0.17103	0.0064
4	5	0.01335	0.04211	0
4	7	0	0.20912	0
4	9	0	0.55618	0
5	6	0	0.25202	0
6	11	0.09498	0.1989	0
6	12	0.12291	0.25581	0
6	13	0.06615	0.13027	0
7	8	0	0.17615	0
7	9	0	0.11001	0
9	10	0.03181	0.0845	0
9	14	0.12711	0.27038	0
10	11	0.08205	0.19207	0
12	13	0.22092	0.19988	0
13	14	0.17093	0.34802	0

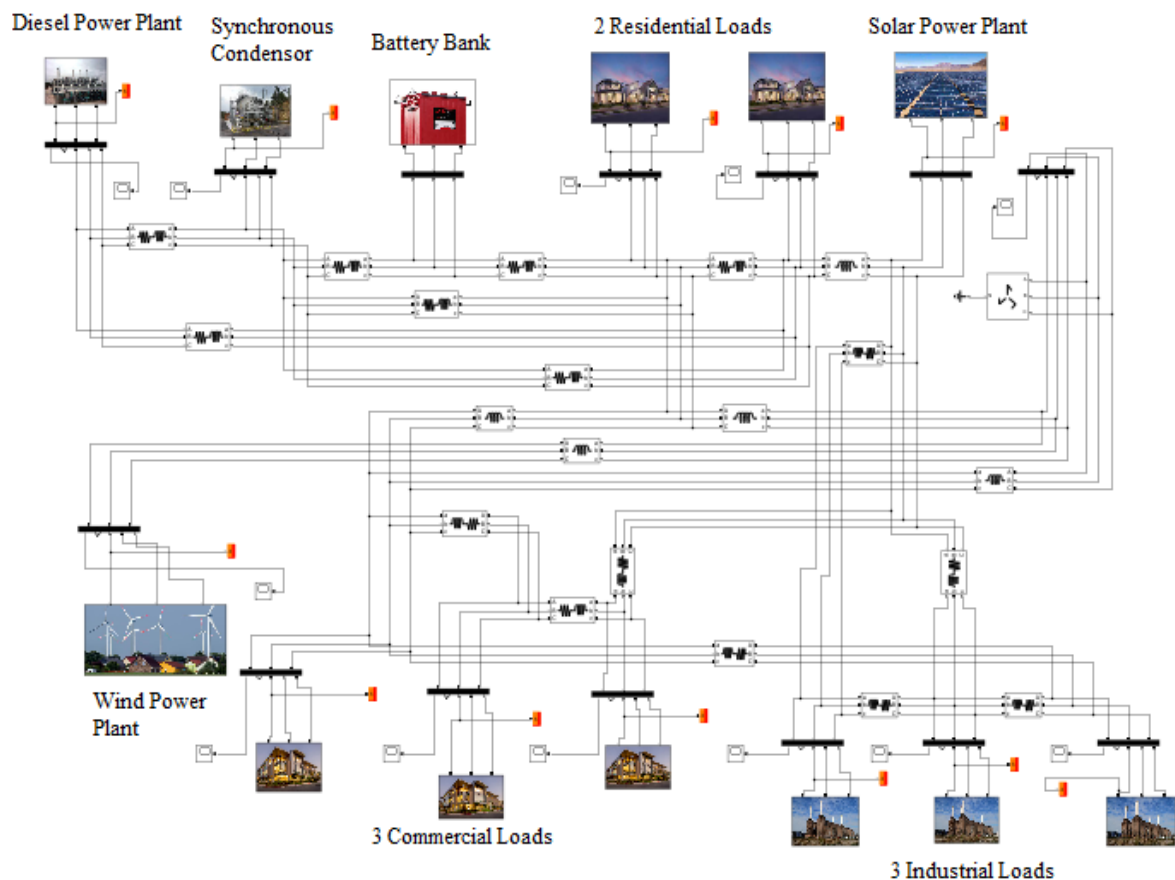


Figure 1. MATLAB/Simulink model of the test model of the microgrid

It consists of the main grid supply which is considered a diesel engine. The main grid has a supply of 10 MVA power and 6.6 kV voltages. Alongside the main grid, wind and solar renewable power models are attached as the secondary power source and a battery is also installed for backup. Wind power has a capacity of 4 MVA power and 575 V voltages, whereas solar power has a capacity of 1 MVA power and 260 V voltages. The battery that is installed has a capacity of 0.5 MVA power and 900 V voltages. For the installation of loads, there are two residential loads, three commercial loads, and three industrial loads each of different specifications. The residential loads consist of three-phase load and single-phase load. The commercial load mainly consists of a three-phase load and the industrial load consists of a three-phase load and an asynchronous machine for representing heavy machinery loads. To compensate for the reactive power in the system a 1 MVA synchronous compensator is also installed. A grounding transformer is also installed for the grounding of the system. The grid is designed at a standard 11 KV voltages and 50Hz frequency. After the design of the system is completed the result of the output is displayed on scopes. The results mainly include the voltages, current, apparent power, active power, and reactive power on the respective buses. A 24-hour simulation is run on the system. Types of loads are tabulated in Table 2 for simulation. After the simulation of the system, the bus data for both the cases are obtained and are shown in Tables 3 and 4. The bus data given in Tables 3 and 4 is used further in Newton–Raphson and PSO for the analysis of the test model of the microgrid. After observing the results, the next step is to conduct the load flow analysis on the system by the two proposed methods. The proposed technique is shown in the flow chart in Figure 2.

Table 2. Types of loads used for simulation

Type of Load	Single Phase/Three Phase	Active Power Load (KW)	Reactive Power Load (KVAR)
Residential [Static]	Single Phase Load [220 V]	1500	3
Residential [Static]	Three Phase Load [440 V]	1000	100
Commercial [Static]	Three Phase Load [440 V]	1000	1
Commercial [Static]	Three Phase Load [440 V]	350000	1
Industrial [Static]	Three Phase Load [3.3 kV]	500	-
Industrial [Dynamic]	Three Phase Load [3.3 kV]	476	324

Table 3. Bus data for battery charging

Bus No.	Bus Code	V (pu)	Load		Generation			
			MW	MVAR	MW	MVAR	Qmin	Qmax
1	1	1	0.0	0.0	0.0	0.0	0.0	0.0
2	2	1	0.0	0.0	0.0	0.0	-inf	inf
3	3	1	0.50	0.0	0.0	0.0	0.0	0.0
4	3	1	0.55	0.06	0.0	0.0	0.0	0.0
5	3	1	0.55	0.06	0.0	0.0	0.0	0.0
6	2	1	0.0	-0.01	0.5	0.0	-inf	inf
7	3	1	0.0	0.0	0.0	0.0	0.0	0.0
8	2	1	0.01	-0.30	2.0	0.0	-inf	inf
9	3	1	0.745	0.0	0.0	0.0	0.0	0.0
10	3	1	0.745	0.0	0.0	0.0	0.0	0.0
11	3	1	0.745	0.0	0.0	0.0	0.0	0.0
12	3	1	1.05	0.4	0.0	0.0	0.0	0.0
13	3	1	1.05	0.4	0.0	0.0	0.0	0.0
14	3	1	1.05	0.4	0.0	0.0	0.0	0.0

Table 4. Bus data for battery supplying

Bus No.	Bus Code	V (pu)	Load		Generation			
			MW	MVAR	MW	MVAR	Qmin	Qmax
1	1	1	0.0	0.0	0.0	0.0	0.0	0.0
2	2	1	0.0	0.0	0.0	0.0	-inf	inf
3	3	1	0.0	0.0	0.5	0.0	-inf	inf
4	3	1	0.55	0.06	0.0	0.0	0.0	0.0
5	3	1	0.55	0.06	0.0	0.0	0.0	0.0
6	2	1	0.0	-0.01	0.5	0.0	-inf	inf
7	3	1	0.0	0.0	0.0	0.0	0.0	0.0
8	2	1	0.01	-0.30	2.0	0.0	-inf	inf
9	3	1	0.745	0.0	0.0	0.0	0.0	0.0
10	3	1	0.745	0.0	0.0	0.0	0.0	0.0
11	3	1	0.745	0.0	0.0	0.0	0.0	0.0
12	3	1	1.05	0.40	0.0	0.0	0.0	0.0
13	3	1	1.05	0.40	0.0	0.0	0.0	0.0
14	3	1	1.05	0.40	0.0	0.0	0.0	0.0

** Angle degrees for all the buses in the 14-bus system is 0° and injected MVAR is also 0

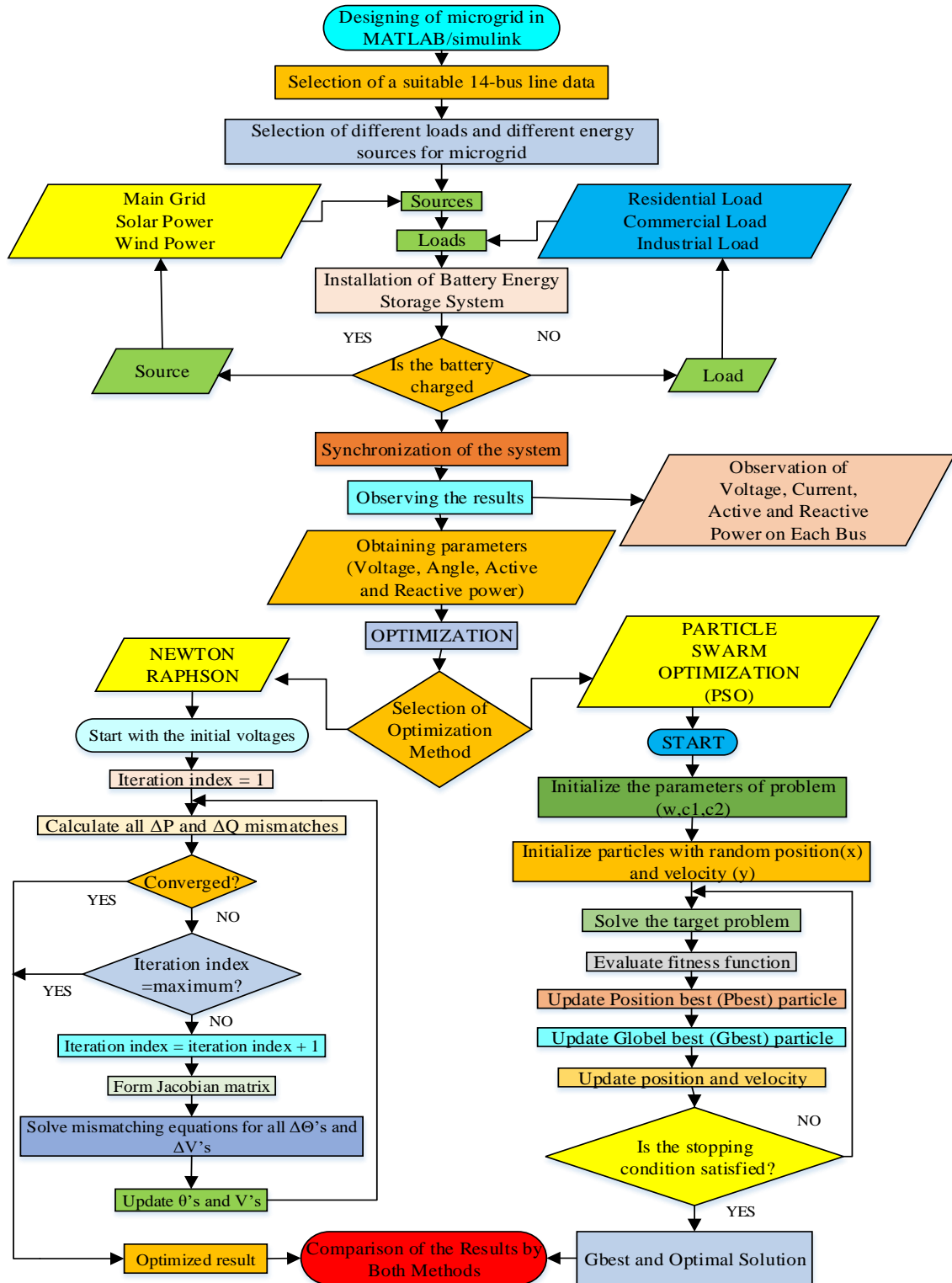


Figure 2. Flow chart of proposed technique

4. SIMULATION RESULTS

After the construction and simulation of the microgrid, the optimal power flow of the system is analyzed. Newton–Raphson and PSO are applied for power flow analysis. This analysis helps to determine the efficacy of Newton–Raphson and PSO in the case of microgrids as microgrids are the most vulnerable power system.

4.1. 24-hour simulation

The determination of the test model's realistic behavior is aided by the 24-hour simulation. Under a 24-hour simulation, various parameters are seen that show how the microgrid test model is doing. This simulation helps in the load forecasting. Following a 24-hour simulation, the microgrid's total apparent power, active power, and reactive power were compared to the total load as follows.

4.1.1. Battery charging

The results for the case of battery charging after a 24-hour simulation of the system are shown in Figure 3. It is quite obvious that a change in apparent power is observed. This observation results in a change in active power because of the increase in power as the battery is charging. The non-uniformity depicts the change in solar irradiance during 24-hours.

4.1.2. Battery discharging

The result for the case of battery discharging after a 24-hour simulation of the system is shown in Figure 4. It is quite obvious that a change in apparent power of the compensator is observed resulting in a change in maintaining the battery power cycle in discharging mode. The non-uniformity shows the 24-hour fluctuation in load. This enables the electrical engineers to apply demand side integration options like peak shaving and peak shifting.

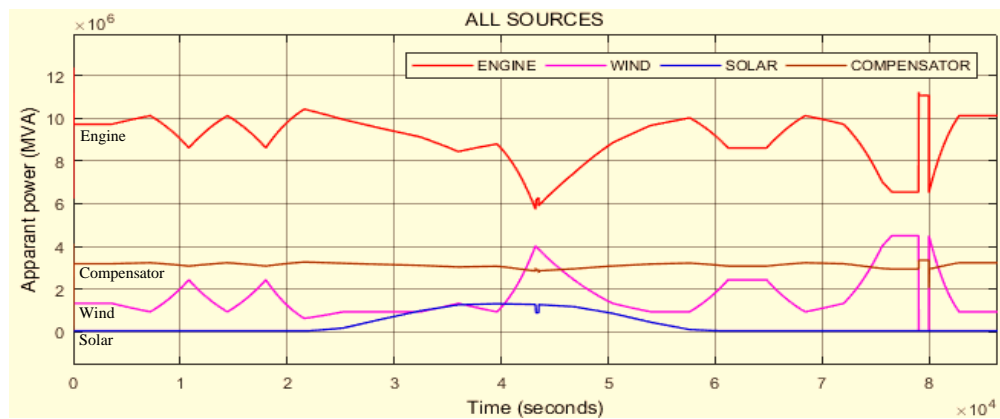


Figure 3. The apparent power of the proposed microgrid test model in the case of battery charging

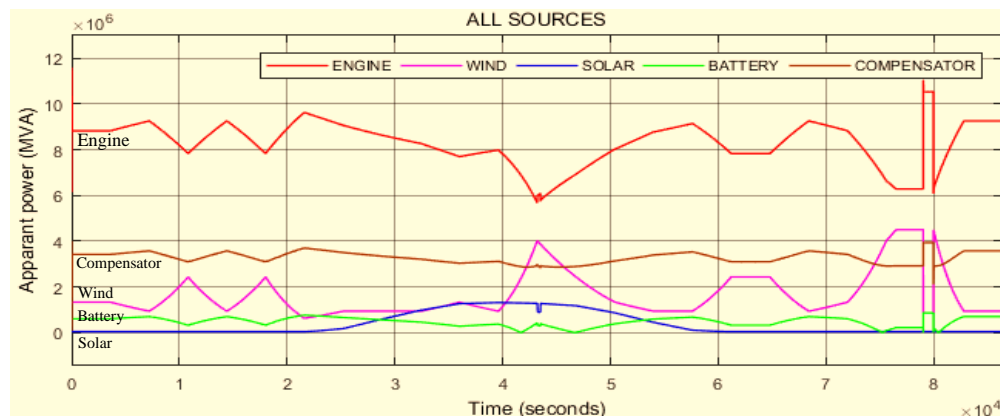


Figure 4. The apparent power of the proposed microgrid test model in the case of battery discharging

4.2. Optimal power flow using Newton–Raphson method

Power flow analysis of the test model of the microgrid is conducted by the Newton–Raphson method. Newton–Raphson method is no doubt, complex but is more accurate. Therefore, promising, and realistic results can be analyzed under different states of battery. There are two cases: battery charging and battery supplying.

4.2.1. Battery charging

The results of the load flow analysis for the case of battery charging conducted by the Newton–Raphson method are presented in Table 5. This study shows the battery charging under the conditions of total available generation and load. Further, total losses of the system and transmission line are tabulated to increase the realism of test model. The voltage profile and angle at each bus are given in Table 6. It is interesting to observe that the values on different buses are closed to 1 p.u. which depicts the reduction in voltage drop.

4.2.2. Battery discharging

The results of the load flow analysis for the case of the battery supplying conducted by the Newton–Raphson method are shown in Table 7. The battery discharging is demonstrated in this study under the circumstances of total available generation and load. To further strengthen the test model's realism, the system and transmission line's total losses are calculated. The voltage profile along with the angle at each bus is presented in Table 8. It is noteworthy to note that the readings on various buses are near to 1 p.u., showing a decrease in voltage loss.

Table 5. N-R based load flow results in the case of battery charging

Parameters	P (MW)	Q (MVAR)
Total Generation	7.183257	1.905875
Total Load	7.155849	1.142204
Total Losses	0.027408	0.763675
Total Transmission Line Losses	0.008771757	0.0479528

Table 6. Voltage profile after N-R based load flow analysis in the case of battery discharging

Bus	Voltage (pu)	Angle
1	1.000	0.00
2	1.000	-32.23
3	0.997	-64.03
4	0.995	-3.77
5	0.995	-3.76
6	1.000	-3.76
7	0.998	-32.35
8	1.000	-61.05
9	0.992	-7.10
10	0.992	-7.15
11	0.992	-7.19
12	0.964	-6.62
13	0.964	-6.60
14	0.964	-6.60

Table 7. N-R based load flow results in the case of battery discharging

Data	P(MW)	Q(MVAR)
Total Generation	6.671125	1.858297
Total Load	6.645655	1.130705
Total Losses	0.02547	0.727589
Total Transmission Line Losses	0.007636	0.043698

Table 8. Voltage profile after N-R based load flow analysis in the case of battery discharging

Bus	Voltage (pu)	Angle
1	1.000	0.00
2	1.000	-32.30
3	1.000	-6.67
4	0.995	-3.83
5	0.995	-3.83
6	1.000	-31.46
7	0.998	-32.42
8	1.000	-61.11
9	0.992	-7.16
10	0.992	-7.21
11	0.991	-7.26
12	0.964	-6.69
13	0.964	-6.67
14	0.964	-6.67

4.3. Optimal power flow using particle swarm optimization

PSO technique is developed and implemented on test model of microgrid. Optimal power flow with low losses is the ultimate goal of PSO. In this test model, the optimization technique is applied under both conditions of battery. The parameters of PSO are initialized and load flow analysis is conducted for both cases.

4.3.1. Battery charging

The results of the load flow analysis for the case of battery charging conducted by the PSO method are listed in Table 9. This study illustrates how batteries charge when total available generation and load are present. To make the test model more realistic, overall losses for the system and transmission line are also recorded. The voltage profile and degree angle at each bus are given in Table 10. It is noteworthy to note that the readings on various buses are near to 1 p.u., showing a decrease in voltage loss.

Table 9. PSO based load flow results in the case of battery charging

Data	P (MW)	Q (MVAR)
Total Generation	7.0157	1.0449
Total Load	6.995	1.01
Total Losses	0.0207	0.0349
Total Transmission Line Losses	0.007285972	0.039819491

Table 10. Voltage profile after PSO based load flow analysis in the case of battery charging

Bus	Voltage (pu)	Angle
1	1.000444212	0
2	0.999668042	-0.001833821
3	0.999790156	-0.003588068
4	1.000014568	-0.004315945
5	1.000476962	-0.004311617
6	1.00174495	-0.00958338
7	0.999792319	-0.005677456
8	0.99909072	-0.003129579
9	1.000118739	-0.007983197
10	1.000106766	-0.009022192
11	1.000582962	-0.010000748
12	0.999649939	-0.011156217
13	0.99999989	-0.010741618
14	0.998737239	-0.010415601

4.3.2. Battery discharging

The results of the load flow analysis for the case of battery charging conducted by the PSO method are shown in Table 11. In this study, the battery discharging is illustrated under the conditions of total available generation and load. The overall losses of the system and transmission line are computed to increase the realism of the test model. The voltage profile and degree angle at each bus are shown in Table 12. It is important to observe that measurements on different buses are close to 1 p.u., indicating a reduction in voltage loss.

4.4. Comparison between Newton–Raphson and particle swarm optimization

In this research, Newton–Raphson method and PSO are implemented on the test model of microgrid. Both the techniques give the fruitful results. However, it is always preferred to pick such technique of power flow analysis that depicts optimal values of voltage and power. Therefore, the comparison is done for voltage profile and transmission line losses for both cases i.e., the battery charging and battery supplying.

Table 11. PSO based load flow results in the case of battery discharging

Data	P (MW)	Q (MVAR)
Total Generation	6.5095	1.0348
Total Load	6.495	1.01
Total Losses	0.0145	0.0248
Total Transmission Line Losses	0.006094745	0.035409565

Table 12. Voltage profile after PSO based load flow analysis in the case of battery discharging

Bus	Voltage (pu)	Degree
1	1.000159538	0
2	0.999033633	-0.001693774
3	1.002852501	-0.003958966
4	0.999333256	-0.004467244
5	0.999786509	-0.004296499
6	1.00178233	-0.00995473
7	0.999831126	-0.006702637
8	0.999333256	-0.005302621
9	1.000101396	-0.008752046
10	1.000095321	-0.009721462
11	1.000591881	-0.01053982
12	0.999687755	-0.011556337
13	1.000026593	-0.011170053
14	0.998737852	-0.011036151

4.4.1. Battery charging

A comparison of voltage profile obtained after load flow analysis by Newton–Raphson method and PSO method is presented in Table 13 in the case of battery charging. This tabular information is further elaborated by graphical analysis, given in Figure 5. It is observed from the results that the voltage profile is more stable in the case of PSO as compared to the Newton–Raphson method for a microgrid system. The utilization of useful power is enhanced with the PSO in the case of battery charging, making microgrid test model a promising model for bidirectional power flow. The comparison of transmission line losses obtained by the Newton–Raphson method and PSO method for the case of battery charging is presented in Table 14 and in Figure 6.

Table 13. Comparison of voltage profile in the case of battery charging

Bus	Newton–Raphson Method	PSO
1	1	1.000444212
2	1	0.999668042
3	0.997	0.999790156
4	0.995	1.000014568
5	0.995	1.000476962
6	1	1.00174495
7	0.998	0.999792319
8	1	0.99909072
9	0.992	1.000118739
10	0.992	1.000106766
11	0.992	1.000582962
12	0.964	0.999649939
13	0.964	0.99999989
14	0.964	0.998737239

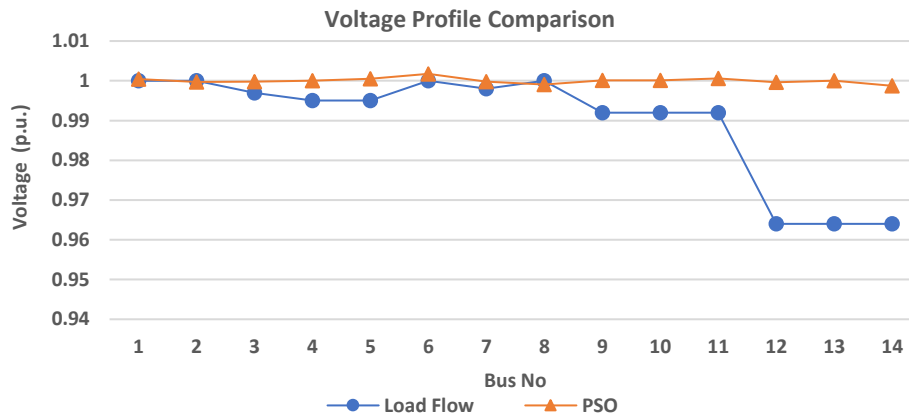


Figure 5. Comparison graph for voltage profile in the case of battery charging

Table 14. Comparison of transmission line losses in the case of battery charging

Data	Active power (MW)	Reactive power (MVAR)
Load Flow	0.008771757	0.04795282
PSO	0.007285972	0.039819491

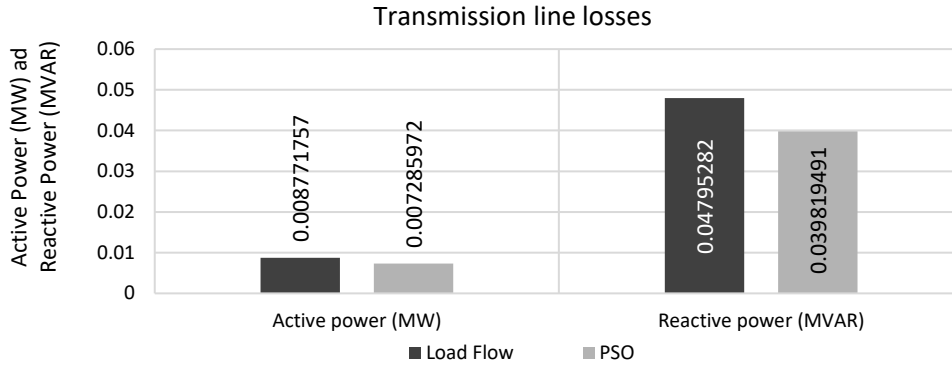


Figure 6. Comparison graph for transmission line losses obtained in the case of battery charging

4.4.2. Battery discharging

The battery serves as a voltage booster in the microgrid system. This is depicted from the tabular presentation of comparison of voltage profiles obtained by Newton–Raphson method and PSO in Table 15. This is further elaborated by the comparison graph, given in Figure 7. Tabular and graphical presentations of transmission line losses are given in Table 16 and Figure 8, respectively.

Table 15. Comparison of voltage profile obtained in the case of battery discharging

Bus	Load Flow	PSO
1	1	1.000159538
2	1	0.999033633
3	1	1.002852501
4	0.995	0.999333256
5	0.995	0.999786509
6	1	1.00178233
7	0.998	0.999831126
8	1	0.999333256
9	0.992	1.000101396
10	0.992	1.000095321
11	0.991	1.000591881
12	0.964	0.999687755
13	0.964	1.000026593
14	0.964	0.998737852

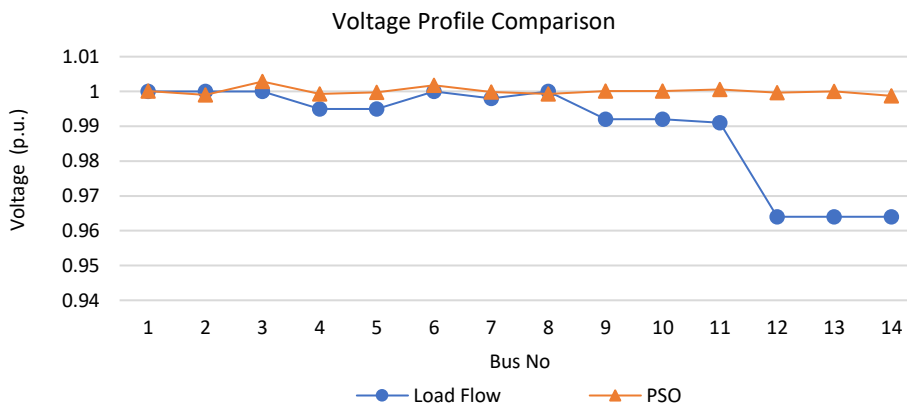


Figure 7. Comparison graph of voltage profiles in the case of battery discharging

Table 16. Comparison of transmission line losses in the case of battery discharging

Data	Active power (MW)	Reactive power (MVAR)
Load Flow	0.007636489	0.043698158
PSO	0.006094745	0.035409565

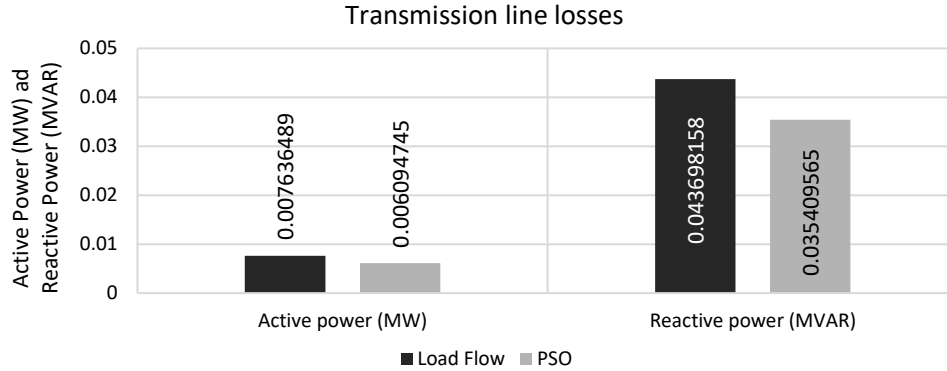


Figure 8. Comparison graph for transmission line losses in the case of battery discharging

5. SIGNIFICANCE OF RESULTS AND SIMULATIONS

Based on the graphical and tabular results, it is found that a significance improvement in the profile of voltage is observed under the battery states of charging and discharging with PSO. It is proven that the transmission line losses are greatly improved with PSO as compared to conventional Newton–Raphson technique. These results open the doors of remodeling of transmission lines under the consideration of available losses and loading. Further, these results enable the national grids to interconnect more renewable energy sources without compromising on voltage profile.

6. PERFORMANCE COMPARISON OF DIFFERENT POWER FLOW TECHNIQUES

In this research, a microgrid test system is analyzed for power flow with Newton–Raphson method and PSO techniques. It has been found from the simulations that voltage profile remains almost closed to 1 p.u. in the case of PSO. This information establishes the reduction in the transmission line losses. From the above-mentioned scenarios of battery charging and discharging, it is observed that transmission line active and reactive power losses are reduced to about 17% in the case of battery charging and 19 to 20% in the case of battery discharging. Table 17 provides a detailed comparison of power flow techniques applied for microgrids.

Table 17. Comparison of different power flow techniques for microgrids

Parameters	Linear Programming	Genetic Programming	Proposed Method
Convergence	Convergence reduces as the power system grows	Convergence reduces as the power system grows but it converges quickly as compared to linear programming	Converges readily in the case of expansion of power system.
Speed	Quick results in the case of simple systems	Relatively quick results in the case of complex systems.	Speedy convergence in the case of complex and complicated results.
Accuracy	Accuracy is compromised in the case of big systems	Accuracy is challenged in the case of expansion of power systems	Accuracy is independent of the system complexities.
Large power systems	Not recommended	Not recommended	Highly recommended
Computational time	High in case of large power systems	High	Less
Computational efforts	Less	High	High

7. CONCLUSION

In this research, a microgrid test model is simulated for an IEEE-14 bus system in MATLAB/Simulink. This test model is incorporated with renewable energy sources to increase the utilization of green energy. Moreover, an energy storage component is also added to the test model. The behavior of the test model is studied under the conditions of charging and discharging of energy storage

devices. Compensating components aid the storage devices to retain their cycle in 24 hours, thus enabling voltage stability for the end-users. In addition to this, optimal power flow is done by the Newton–Raphson method and PSO. It is found from the comparison that utilization of active power is more effective with the implementation of PSO as compared to the Newton–Raphson method. As a result, a more stable voltage profile is obtained with enhanced power transfer capacity by decreasing the transmission line losses. This study builds an argument to motivate small-scale enterprises in Pakistan and developing countries to adopt green energy policy. This will not only be environmentally friendly but also make the world safe for future generations.

ACKNOWLEDGEMENTS

The authors are thankful to the Department of Electrical Engineering, University of Lahore, Lahore, Pakistan, Department of Computer Science, University of Skövde, Sweden, Department of Electrical Engineering, Comsats Institute of Information Technology (CIIT), Lahore, Pakistan and Department of Technology, University of Lahore, Lahore, Pakistan for providing facilities to research Microgrids.

REFERENCES

- [1] H. Kaur, Y. S. Brar, and J. S. Randhawa, "Optimal power flow using power world simulator," in *2010 IEEE Electrical Power and Energy Conference*, Aug. 2010, pp. 1–6, doi: 10.1109/EPEC.2010.5697188.
- [2] J. M. Andujar, F. Segura, and T. Dominguez, "Study of a renewable energy sources-based smart grid. requirements, targets and solutions," in *2016 3rd Conference on Power Engineering and Renewable Energy (ICPERE)*, 2016, pp. 45–50, doi: 10.1109/ICPERE.2016.7904849.
- [3] M. N. Hidayat and F. Li, "Implementation of renewable energy sources for electricity generation in Indonesia," in *2011 IEEE Power and Energy Society General Meeting*, Jul. 2011, pp. 1–4, doi: 10.1109/PES.2011.6039326.
- [4] K. Anoune, M. Bouya, M. Ghazouani, A. Astito, and A. Ben Abdellah, "Hybrid renewable energy system to maximize the electrical power production," in *2016 International Renewable and Sustainable Energy Conference (IRSEC)*, Nov. 2016, pp. 533–539, doi: 10.1109/IRSEC.2016.7983992.
- [5] N. A. Ahmed, M. Miyatake, and A. K. Al-Othman, "Power fluctuations suppression of stand-alone hybrid generation combining solar photovoltaic/wind turbine and fuel cell systems," *Energy Conversion and Management*, vol. 49, no. 10, pp. 2711–2719, Oct. 2008, doi: 10.1016/j.enconman.2008.04.005.
- [6] IEA, "Renewable energy outlook 2013," *International Energy Agency*, 2013. Accessed: Jun. 03, 2022. [Online]. Available: <https://iea.blob.core.windows.net/assets/a22dedb8-c2c3-448c-b104-051236618b38/WEO2013.pdf>
- [7] P. García, J. P. Torreglosa, L. M. Fernández, and F. Jurado, "Optimal energy management system for stand-alone wind turbine/photovoltaic/hydrogen/battery hybrid system with supervisory control based on fuzzy logic," *International Journal of Hydrogen Energy*, vol. 38, no. 33, pp. 14146–14158, Nov. 2013, doi: 10.1016/j.ijhydene.2013.08.106.
- [8] M. F. Aziz and N. Abdulaziz, "Prospects and challenges of renewable energy in Pakistan," in *2010 IEEE International Energy Conference*, Dec. 2010, pp. 161–165, doi: 10.1109/ENERGYCON.2010.5771667.
- [9] Z. Umrani, "Solar energy: Challenges and opportunities in Pakistan," in *2017 International Conference on Innovations in Electrical Engineering and Computational Technologies (ICIEECT)*, Apr. 2017, pp. 1–1, doi: 10.1109/ICIEECT.2017.7916603.
- [10] S. Kanwa, B. Khan, and M. Qasim Rauf, "Infrastructure of sustainable energy development in Pakistan: A review," *Journal of Modern Power Systems and Clean Energy*, vol. 8, no. 2, pp. 206–218, 2020, doi: 10.35833/MPCE.2019.000252.
- [11] A. K. Sandhu and A. Fatima, "Integrating renewable energy policies and sustainable development tools for the assessment of policy reforms," in *2014 International Conference on Energy Systems and Policies (ICESP)*, Nov. 2014, pp. 1–6, doi: 10.1109/ICESP.2014.7347009.
- [12] J. Vasquez, J. Guerrero, J. Miret, M. Castilla, and L. Garcia de Vicuna, "Hierarchical control of intelligent microgrids," *IEEE Industrial Electronics Magazine*, vol. 4, no. 4, pp. 23–29, Dec. 2010, doi: 10.1109/MIE.2010.938720.
- [13] R. Majumder, A. Ghosh, G. Ledwich, and F. Zare, "Power management and power flow control with back-to-back converters in a utility connected microgrid," *IEEE Transactions on Power Systems*, vol. 25, no. 2, pp. 821–834, May 2010, doi: 10.1109/TPWRS.2009.2034666.
- [14] T. K. A. Brekken, A. Yokochi, A. von Jouanne, Z. Z. Yen, H. M. Hapke, and D. A. Halam, "Optimal energy storage sizing and control for wind power applications," *IEEE Transactions on Sustainable Energy*, Jan. 2010, doi: 10.1109/TSTE.2010.2066294.
- [15] R. Muzzammel, "Comprehensive analysis of planning operation and protection of microgrid systems," *Journal of Energy Research and Reviews*, pp. 40–58, Sep. 2020, doi: 10.9734/jenrr/2020/v6i130160.
- [16] R. Muzzammel, R. Arshad, S. Mehmood, and D. Khan, "Advanced energy management system with the incorporation of novel security features," *International Journal of Electrical and Computer Engineering (IJECE)*, vol. 10, no. 4, pp. 3978–3987, Aug. 2020, doi: 10.11591/ijece.v10i4.pp3978-3987.
- [17] Y. M. Atwa, E. F. El-Saadany, M. M. A. Salama, and R. Seethapathy, "Optimal renewable resources mix for distribution system energy loss minimization," *IEEE Transactions on Power Systems*, vol. 25, no. 1, pp. 360–370, Feb. 2010, doi: 10.1109/TPWRS.2009.2030276.
- [18] H. Nikkhajoei and R. Iravani, "Steady-state model and power flow analysis of electronically-coupled distributed resource units," *IEEE Transactions on Power Delivery*, vol. 22, no. 1, pp. 721–728, Jan. 2007, doi: 10.1109/TPWRD.2006.881604.
- [19] A. G. Tsikalakis and N. D. Hatziargyriou, "Centralized control for optimizing microgrids operation," *IEEE Transactions on Energy Conversion*, vol. 23, no. 1, pp. 241–248, Mar. 2008, doi: 10.1109/TEC.2007.914686.
- [20] G. Celli, E. Ghiani, S. Mocci, and F. Pilo, "A multiobjective evolutionary algorithm for the sizing and siting of distributed generation," *IEEE Transactions on Power Systems*, vol. 20, no. 2, pp. 750–757, May 2005, doi: 10.1109/TPWRS.2005.846219.
- [21] S. Singh, D. W. Gao, and J. Giraldez, "Cost analysis of renewable energy-based microgrids," in *2017 North American Power Symposium (NAPS)*, Sep. 2017, pp. 1–4, doi: 10.1109/NAPS.2017.8107241.

- [22] H. Wang, "Investment efficiency and cost analysis of new renewable energy sources," in *2020 IEEE Sustainable Power and Energy Conference (iSPEC)*, Nov. 2020, pp. 1082–1087, doi: 10.1109/iSPEC50848.2020.9351110.
- [23] Y. Levron and D. Shmilovitz, "Power systems' optimal peak-shaving applying secondary storage," *Electric Power Systems Research*, vol. 89, pp. 80–84, Aug. 2012, doi: 10.1016/j.epsr.2012.02.007.
- [24] J. P. Barton and D. G. Infield, "Energy storage and its use with intermittent renewable energy," *IEEE Transactions on Energy Conversion*, vol. 19, no. 2, pp. 441–448, Jun. 2004, doi: 10.1109/TEC.2003.822305.
- [25] Y. Levron and D. Shmilovitz, "Optimal power management in fueled systems with finite storage capacity," *IEEE Transactions on Circuits and Systems I: Regular Papers*, vol. 57, no. 8, pp. 2221–2231, Aug. 2010, doi: 10.1109/TCSI.2009.2037405.
- [26] R. Muzzammel, M. Ahsan, and W. Ahmad, "Non-linear analytic approaches of power flow analysis and voltage profile improvement," in *2015 Power Generation System and Renewable Energy Technologies (PGSRET)*, Jun. 2015, pp. 1–7, doi: 10.1109/PGSRET.2015.7312232.
- [27] D. W. Wells, "Method for economic secure loading of a power system," *Proceedings of the Institution of Electrical Engineers*, vol. 115, no. 8, p. 1190, 1968, doi: 10.1049/piee.1968.0210.
- [28] R. Muzzammel and R. Arshad, "Comprehensive analysis and design of furnace oil-based power station using ETAP," *International Journal of Applied Power Engineering (IJAPE)*, vol. 11, no. 1, pp. 33–51, Mar. 2022, doi: 10.11591/ijape.v11i1.pp33-51.
- [29] R. Muzzammel, I. Khail, M. H. Tariq, A. M. Asghar, and A. Hassan, "Design and power flow analysis of electrical system using electrical transient and program software," *Energy and Power Engineering*, vol. 11, no. 04, pp. 186–199, 2019, doi: 10.4236/epe.2019.114011.
- [30] R. Madani, M. Ashraphijuo, J. Lavaei, and R. Baldick, "Power system state estimation with a limited number of measurements," in *2016 IEEE 55th Conference on Decision and Control (CDC)*, Dec. 2016, pp. 672–679, doi: 10.1109/CDC.2016.7798346.
- [31] R. Muzzammel and H. Ali, "Monte carlo simulation of load flow analysis of power system," *International Journal of Scientific and Engineering Research*, vol. 8, no. 3, pp. 534–537, 2017.
- [32] S. Jaiswal and T. Ghose, "Optimal real power dispatch of centralized micro-grid control operation," in *2017 International Conference on Circuit, Power and Computing Technologies (ICCPCT)*, Apr. 2017, pp. 1–7, doi: 10.1109/ICCPCT.2017.8074196.
- [33] N. K. Mahto, S. Jaiswal, and D. C. Das, "Demand-side management approach using heuristic optimization with solar generation and storage devices for future smart grid," in *Renewable Energy Towards Smart Grid*, 2022, pp. 407–420.
- [34] P. Kumar, A. K. Barik, and D. C. Das, "Comparative study on optimal frequency control of interconnected hybrid microgrid based mini VPP using PSO and SSA," *Journal of Mobile Computing, Communications and Mobile Networks*, vol. 7, no. 1, pp. 7–15, 2020.
- [35] M. S. Syed, S. V. Chintalapudi, and S. Sirigiri, "Optimal power flow solution in the presence of renewable energy sources," *Iranian Journal of Science and Technology, Transactions of Electrical Engineering*, vol. 45, no. 1, pp. 61–79, Mar. 2021, doi: 10.1007/s40998-020-00339-z.
- [36] B. Bhandari, S. R. Poudel, K.-T. Lee, and S.-H. Ahn, "Mathematical modeling of hybrid renewable energy system: A review on small hydro-solar-wind power generation," *International Journal of Precision Engineering and Manufacturing-Green Technology*, vol. 1, no. 2, pp. 157–173, Apr. 2014, doi: 10.1007/s40684-014-0021-4.
- [37] D. Bienstock, M. Escobar, C. Gentile, and L. Liberti, "Mathematical programming formulations for the alternating current optimal power flow problem," *4OR*, vol. 18, no. 3, pp. 249–292, Sep. 2020, doi: 10.1007/s10288-020-00455-w.
- [38] W. Tinney and C. Hart, "Power flow solution by Newton's method," *IEEE Transactions on Power Apparatus and Systems*, vol. PAS-86, no. 11, pp. 1449–1460, Nov. 1967, doi: 10.1109/TPAS.1967.291823.
- [39] M. Abokrishna, A. Diaa, A. Selim, and S. Kamel, "Development of Newton-Raphson power-flow method based on second order multiplier," in *2017 Nineteenth International Middle East Power Systems Conference (MEPCON)*, Dec. 2017, pp. 976–980, doi: 10.1109/MEPCON.2017.8301299.
- [40] H. Le Nguyen, "Newton-Raphson method in complex form [power system load flow analysis]," *IEEE Transactions on Power Systems*, vol. 12, no. 3, pp. 1355–1359, 1997, doi: 10.1109/59.630481.
- [41] M. U. Afzaal *et al.*, "Probabilistic generation model of solar irradiance for grid connected Photovoltaic systems using Weibull distribution," *Sustainability*, vol. 12, no. 6, Mar. 2020, doi: 10.3390/su12062241.
- [42] S. Cheng, Y. Xie, Z. Shu, Y. Wang, Z. Ning, and Y. Yang, "Effect of different solar irradiance parameters on reliability evaluation of the grid," *IOP Conference Series: Earth and Environmental Science*, vol. 300, no. 4, Jul. 2019, doi: 10.1088/1755-1315/300/4/042115.
- [43] J. V. Seguro and T. W. Lambert, "Modern estimation of the parameters of the Weibull wind speed distribution for wind energy analysis," *Journal of Wind Engineering and Industrial Aerodynamics*, vol. 85, no. 1, pp. 75–84, Mar. 2000, doi: 10.1016/S0167-6105(99)00122-1.

BIOGRAPHIES OF AUTHORS



Raheel Muzzammel    received the B.Sc. degree in Electrical Engineering from the University of Engineering and Technology, Lahore, Pakistan in 2010 and the M.S. and Ph.D. degree in Electrical Engineering from the University of Lahore, Lahore, Pakistan in 2013 and 2022, respectively. He is currently working as an Assistant Professor at the University of Lahore, Lahore, Pakistan. His research interests include power system analysis, power system protection, artificial neural networks, power transmission lines, machine learning, microgrids, and smart grids. He can be contacted at raheelmuzzammel@gmail.com.



Rabia Arshad    received the master's degree in electrical engineering from the University of Lahore, Lahore in 2016 following her B.Sc. in computer engineering from the University of Engineering and Technology, Lahore. Currently, he is working as an assistant professor in the Department of Electrical Engineering in the University of Lahore, Lahore, Pakistan. She has an experience of more than 12 years in academia. Her research interests include communication systems and smart grids. She can be contacted at email: rabia.arshad1615@gmail.com.



Sobia Bashir    received a master's degree in computer science from the University of Lahore, Lahore in 2007 following his B.Sc. in computer science from the University of Lahore Pakistan. She has an experience of more than 7 years in academia. Moreover, she worked as a junior software developer at Transoft Solution AB Sweden. Currently, she is pursuing master's in Data Science from the University of Skövde, Sweden. Her research interests include machine learning and computer networks. She can be contacted at email: sobiabashir_786@gmail.com and her ResearchGate ID: <https://www.researchgate.net/profile/Sobia-Bashir-3>.



Uzma Mushtaq    was born in Islamabad, Pakistan. She received her B.S. degree from Air University, Islamabad, Pakistan and MS degree from National University of Science and Technology (NUST), Islamabad, Pakistan in electrical engineering in 2009 and 2012, respectively. She is currently pursuing her Ph.D. from COMSATS Institute of Information Technology (CIIT), Lahore, Pakistan in Electrical Engineering. Since 2016, she is working as an assistant professor in The University of Lahore, Lahore campus, Pakistan. Her research interests include 5G, multicarrier communication networks and digital signal processing. Her profile can be found at <https://www.researchgate.net/profile/Uzma-Mushtaq> and she can be contacted at uzma.mushtaq@tech.uol.edu.pk.



Fariha Durrani     is currently working as a lecturer in Department of Electrical Engineering, University of Lahore. She has done her Master of Science in electrical engineering from The University of Lahore (UOL) in 2015. She has got nine years' experience of teaching various power engineering courses at undergraduate level as well as supervising many semester projects. She has also participated in Faculty Development Workshops and Seminars on Power System. Her research interests include power systems, photo-voltaic systems, power electronics and load management. She can be contacted at fariha.durrani@ee.uol.edu.pk.



Sadaf Noshin    was born in Vehari, Pakistan. She received her B.S. degree from B.Z.U Multan, Pakistan and MS degree from University of Engineering and Technology (UET) Lahore, Pakistan in architectural engineering in 2012 and 2018, respectively. She is currently pursuing her Ph.D. from University of Engineering and Technology (UET) Lahore, Pakistan in architectural engineering. Since 2016, she is working as an assistant professor in The University of Lahore, Lahore campus, Pakistan. Her research interests include energy efficient materials and designs. She can be contacted at email sadaf.noshin@tech.uol.edu.pk and her ResearchGate ID: <https://www.researchgate.net/profile/Sadaf-Noshin>.